GEOPHYSICS, VOL. 86, NO. 3 (MAY-JUNE 2021); P. WA89–WA97, 12 FIGS.
10.1190/GEO2020-0400.1

Distributed acoustic sensing for shallow seismic investigations and void detection

Yarin Abukrat[1] and Moshe Reshef[1]

ABSTRACT

During the past few decades, fiber-optic-based distributed acoustic sensing (DAS) has emerged as an affordable, easy-to-deploy, reliable, and noninvasive technique for high-resolution seismic sensing. We have determined that fiber deployments dedicated to near-surface seismic applications, commonly used for the detection and localization of voids, can be used effectively with conventional processing techniques. We tested a variety of small sources in different geologic environments. These sources, operated on and below the surface, were recorded by horizontal and vertical DAS arrays. Our results and comparisons to data acquired by vertical-component geophones demonstrate that DAS may be sufficient for acquiring near-surface seismic data. Furthermore, we tried to address the issue of directional sensing by DAS arrays and use it to solve the problem of wave-mode separation. Records acquired by a unique acquisition setup suggest that one can use the nature of standard DAS systems as uniaxial strainmeters to record separated wave modes. Finally, we applied two seismic methods on DAS data acquired at a test site: multichannel analysis of surface waves (MASW) and shallow diffraction imaging. These methods allowed us to determine the feasibility of using DAS systems for imaging shallow subsurface voids. MASW was used to uncover anomalies in the S-wave velocity, whereas shallow diffraction imaging was applied to identify the location of the void. The results we obtained illustrate that by using these methods we are able to accurately detect the true location of the void.

DOI:10.1190/geo2020-0400.1

INTRODUCTION

Shallow seismic methods play a major part in near-surface geophysics because they are relatively cost effective and do not require exceptional logistics. In addition, these methods provide a noninvasive way to characterize and image the shallow subsurface with very high resolution. Near-surface seismic techniques have many possible applications in geotechnical engineering, security, hydrology, and archeology. There are various targets for these applications, such as detecting sinkholes that might cause a severe surface collapse in urban areas, searching for contaminated aquifers, and identification of clandestine tunnels.

Many geophysical methods have been applied to study the shallow subsurface, such as gravity (Butler, 1984), microgravity (Rybakov et al., 2001), electromagnetics (Auken et al., 2006), and ground-penetrating radar (GPR) (Cassidy et al., 2011). Seismic methods have also been used, demonstrating that of all of the geophysical methods, it is the most successful and has the highest resolution (Belfer et al., 1998; Sloan et al., 2010). However, in specific geologic settings, especially when investigating ultrashallow depths (i.e., several meters), GPR is expected to yield better results (Lai et al., 2018). Using seismic methods in the shallow subsurface can be very challenging due to the characteristics of the medium that include strong attenuation and high heterogeneity, often of unconsolidated material. These characteristics pose limitations on acquisition layouts, reduce the quality of the source and receiver coupling, and require special attention to wave-mode conversions. As a result, data quality can be poor and standard processing procedures fail. Nevertheless, the size of objects that need to be detected and mapped is usually small and the required accuracy is high.

Distributed acoustic sensing (DAS) is a well-known modern technology of growing interest for seismic applications. DAS uses coherent optical time-domain reflectometry to accurately record seismic wavefields along a fiber-optic (FO) cable at high spatial and temporal resolutions. The FO cable is examined by a laser interrogator unit (IU) that measures the fiber's response to strain caused

Manuscript received by the Editor 9 June 2020; revised manuscript received 9 February 2021; published ahead of production 10 March 2021; published online 21 April 2021.
[1]Tel Aviv University, Raymond and Beverly Sackler Faculty of Exact Sciences, Department of Geophysics, Tel Aviv 69978, Israel. E-mail: yarinabukrat@mail.tau.ac.il (corresponding author); mosher@tauex.tau.ac.il.

by interactions with seismic waves. Compared with conventional geophones, DAS has several inherent advantages. First, FO cables are distributed sensors that can be deployed continuously over large distances in vertical and horizontal configurations, whereas geophones are point sensors with limited coverage that depends on their quantity (Parker et al., 2014). Second, DAS can be deployed in places inaccessible to geophones or where geophones might not be safely deployed, such as slim-hole wells or long horizontal wells (Mestayer et al., 2011). Third, once an FO cable has been installed, DAS data can be acquired at any time by bringing an IU and a source with no further intervention. This provides an easy method for long-term seismic monitoring that dramatically saves the cost and logistics of the invasive geophones' deployment. Thus, DAS enables nonintrusive, on-demand seismic acquisition more affordably than conventional acquisition, especially offshore. Moreover, existing FO cables, which are widespread in urban areas for telecommunication (Dou et al., 2017; Martin et al., 2017), and can also be found in wells for measuring temperature and pressure, can be used for DAS (Mateeva et al., 2013, 2014). During the past few decades, DAS has been used, inter alia, for onshore and offshore vertical seismic profiling (VSP) (Mestayer et al., 2011; Daley et al., 2013; Mateeva et al., 2013, 2014), earthquake seismology (Lindsey et al., 2017; Lellouch et al., 2019), and seismic monitoring (Karrenbach et al., 2017). However, despite the variety of geophysical applications of DAS arrays, little attention has been paid to use them to detect near-surface voids.

Working with separate P- and S-waves in the shallow subsurface has many advantages, such as improving voids' imaging quality by focusing the S-wave diffractions. These S-wave events are often the most powerful and coherent component of the backscattered wavefield (Lellouch and Reshef, 2017; Peterie et al., 2020). In addition, it enhances elastic waveform inversion schemes (Wang et al., 2002) and yields information regarding different rock properties such as lithology, porosity, and anisotropy (Barkved et al., 2004). Various authors have proposed methods for separating P- and S-wavefields including working in the τ-p domain (i.e., intercept time-slowness domain) (Greenhalgh et al., 1990), working in the f-k domain (i.e., frequency-wavenumber domain) (Dankbaar, 1987), and by singular-value decomposition (Kendall et al., 2005). However, an optimal separation should be obtained by designing a proper acquisition setup.

In the following, we test different scenarios of using DAS for seismic exploration of the shallow subsurface. We emphasize the importance of using the tested methods for void detection and localization. Comparisons with standard geophones will be presented together with considerations for placing horizontal and vertical arrays used to check the ability to separate different wave modes. Finally, we demonstrate the use of 2D DAS field data to accurately image a real subsurface void.

FIELD OPERATIONS AND TEST SITES DESCRIPTION

The data presented in this paper were acquired at two areas having different geologic settings — area A and area B. Area A is characterized by relatively high seismic velocities due to the widely exposed carbonates in this region. Area B, on the other hand, has mainly sandy shales in the shallow subsurface, which are indicated by relatively low velocities. In general, the velocities in area B are 5–10 times slower than those observed in area A.

A noncommercial IU, connected to a standard, single-mode FO cable was used to record all of the DAS data analyzed in this study. This DAS system uses Rayleigh backscattering and measures the strain along the fiber. We used a sampling frequency of 1 kHz and a gauge length of 10 m. The gauge length is a spatial distance over which the strain is measured, and it must not be confused with the DAS channel spacing (Dou et al., 2017). Although we used a time-zero trigger to record some of the gathers during the experiments, most of the data were recorded continuously. The displayed seismograms were extracted around the analyzed events from the nontriggered data. As will be shown in the following, most acquisition layouts were over distances of no more than 150–200 m and depths of 45 m. When geophones were placed right above the trenched fiber, we verified that they were practically unaffected by the underlying trench.

OPTIMIZING THE HORIZONTAL DAS ARRAY LAYOUT

The most convenient and cost-effective procedure to detect and locate subsurface voids is by acquiring seismic data on the surface. Traditionally, this is done by using a surface source and a set of geophones, deployed on the surface. To evaluate the usability of DAS for this basic operation, we compared geophone and DAS data. Figure 1 displays data acquired at area A using standard 25 Hz vertical-component geophones and a DAS array, both positioned along the same surface line. The geophone data were recorded by a spread of 48 geophones positioned on a moderately rugged ground surface, whereas the DAS data were recorded by a 48-station DAS array buried 0.5 m below the surface. A 5 kg sledgehammer striking a steel plate was used as a vertical impact source, and the group spacing was 1 m for both data types. The dominant frequency of the geophone data is significantly higher than the dominant frequency of the DAS data, making the appearance of the seismic events very different. Moreover, the traces occupying the near offsets of the DAS data are highly disturbed and suffer from a lack of coherency, whereas the geophone data show coherent events even at the very near offsets. This is a result of applying the source right above the trench where the fiber was placed.

When operating over a less rugged surface, combined with a lightly disturbed shallow subsurface, the quality of the DAS data is highly improved. Figure 2b presents a shot record acquired at area B by a 200-station DAS array, buried in a trench of 0.5 m depth. The 5 kg sledgehammer source was activated on the surface 15 m away from the DAS array (see Figure 2a). This resulted in an improved quality of the near-offset traces. All of the different direct arrival waves, including the prominent surface waves, are clearly observed. However, by inspecting the amplitude spectrum of the seismogram, the dominant frequency still remains low (see Figure 2c), even for these ideal acquisition conditions.

When we extend the distance between the source and the DAS array, a more complicated seismogram is obtained. Figure 3 shows the result of recording the 5 kg sledgehammer source in area B. Several surface shots were located approximately 75 m away from the center of the DAS array (see Figure 3a). No trigger was used in this experiment. Other than the nonsymmetric first arrival, it is very difficult to identify the specific events that have been recorded. Backscattered energy, from a subsurface void that will arrive during the time gate of these complicated direct arrivals (see Figure 3c), will be almost impossible to detect. A noticeable "line" across

DOI:10.1190/geo2020-0400.1

which phase changes of the recorded wavefield occur can be seen where the fiber is perpendicular to the source. This phase change is a result of the fiber straining in opposite directions along its axis. To further investigate the nature of this phase change, a more detailed, nontriggered experiment was conducted at area B (see Figure 4). To suppress the effect of the surface waves, a directional impact source was applied at a depth of 10 m. The seismogram recorded by a short DAS array, located in a 0.5 m deep trench, is compared to a similar seismogram, recorded by a set of 5 Hz vertical-component geophones, located on the surface, right above the fiber. The source operated in a direction almost perpendicular to the recording arrays vis-à-vis their center. In Figure 4b, a clear phase change can be identified across the event on the DAS seismogram, as opposed to the geophone data in Figure 4c. To better separate between the P- and S-waves, the seismograms from a similar experiment, in which the source was applied at a larger distance (see Figure 4d), are shown in Figure 4e and 4f. The sharp phase change of these two events can be seen only on the DAS data (Figure 4e). In addition, comparing Figure 4b and 4c with Figure 4e and 4f indicates that when the source is activated at a greater distance, the data contain significantly lower frequencies as opposed to when activated from a closer distance. If we consider the first event to be the P-wave and the

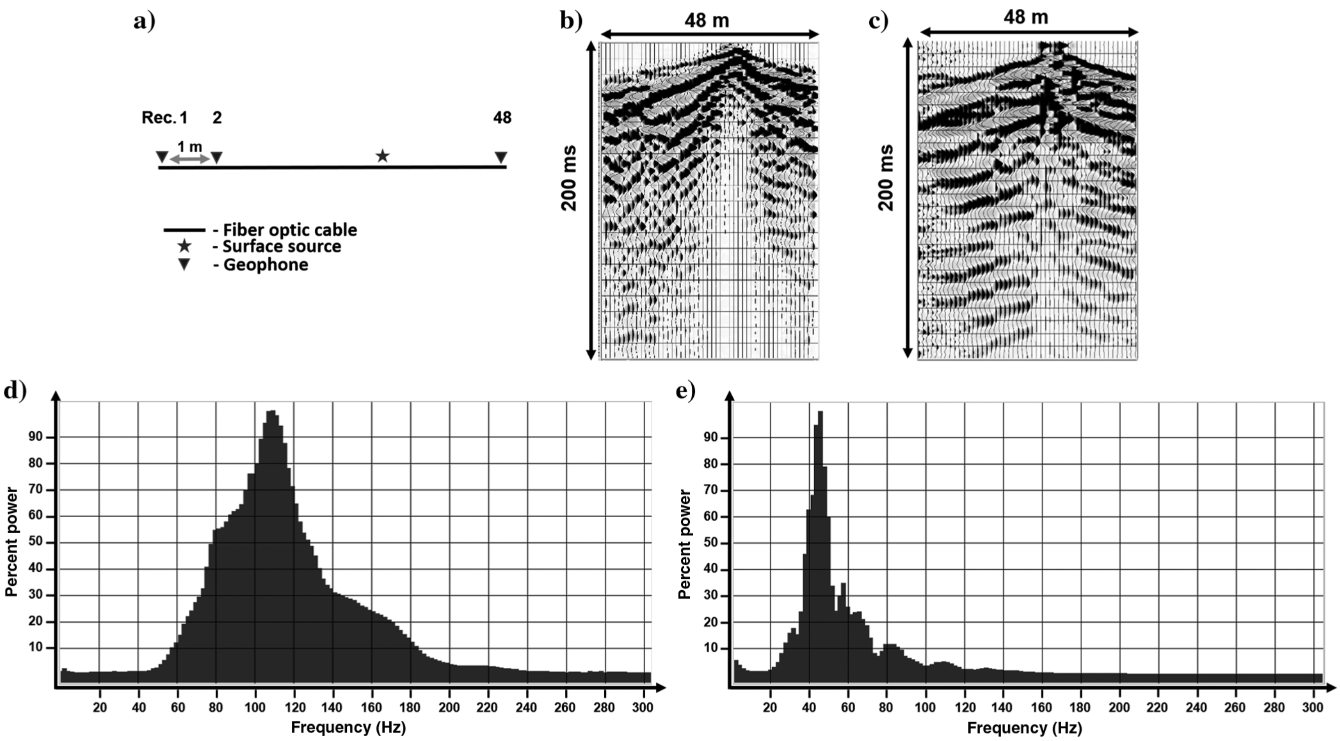

Figure 1. A comparison of geophone and DAS data. (a) A map view of the acquisition setup. Shot records acquired by (b) an array of 25 Hz geophones and (c) a DAS array. Power spectra of the (d) geophone and (e) DAS shot records.

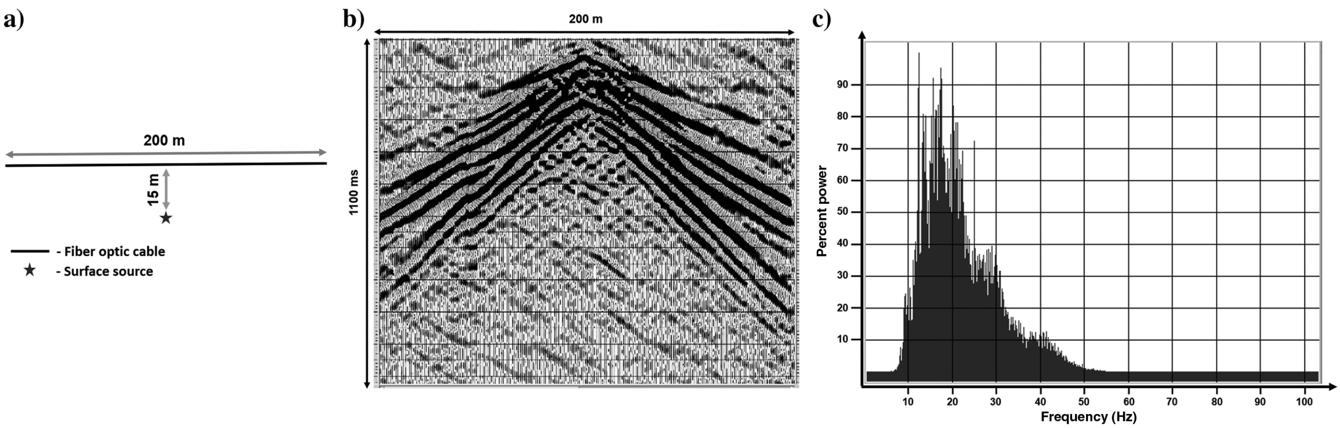

Figure 2. (a) A map view of the acquisition setup. (b) A shot record acquired with a DAS array and (c) its corresponding power spectrum.

DOI:10.1190/geo2020-0400.1

second one to be the S-wave, then the source orientation suggests that we are looking at the vertical component of the S-wave (SV). Assuming minor lateral velocity variation, this sharp phase change on the DAS data could be used as a horizontal directional pointer to a primary or secondary subsurface source.

Near-surface void detection has been reported to favor the use of S-waves and, in particular, SH-waves. Ideally, a directional or a shear-source and a 3C recording system should be used for data acquisition (Lellouch and Reshef, 2017; Peterie et al., 2020). To test the possibility of differentiating between the wave types using a horizontally trenched fiber, we set an experiment at area A (see Figure 5a). The depth of the DAS trench was 0.5 m, and a directional impact source was placed approximately 20 m below the surface. When we examine the nontriggered seismogram in Figure 5b, two clear first-arrival events can be observed. The slight delay of the event on the right and the distinct difference between the slope of the events suggest that these are P- (b to c on the seismogram) and SH-waves (b to a on the seismogram). The approximate velocities of the events are in agreement with known velocities in the experiment's region.

VERTICAL DAS ARRAY

Vertical DAS arrays have been successfully used over the past few decades for oil and gas exploration, earthquake seismology, seismic monitoring, and more. From an operational point of view, the placement of the fiber in boreholes is more complicated, but for studying the shallow subsurface, the drilling operation may become a reasonable task. Void detection using VSP, reverse VSP, or cross-well operations can avoid many of the deficiencies associated with standard surface seismic data (Shustak et al., 2015; Lellouch and Reshef, 2017). Here, we try to examine the possibility of using standard DAS equipment and recording parameters to operate in shallow boreholes.

The results of a simple field test, done at area B, are displayed in Figure 6. The DAS array is continuous between points a and d,

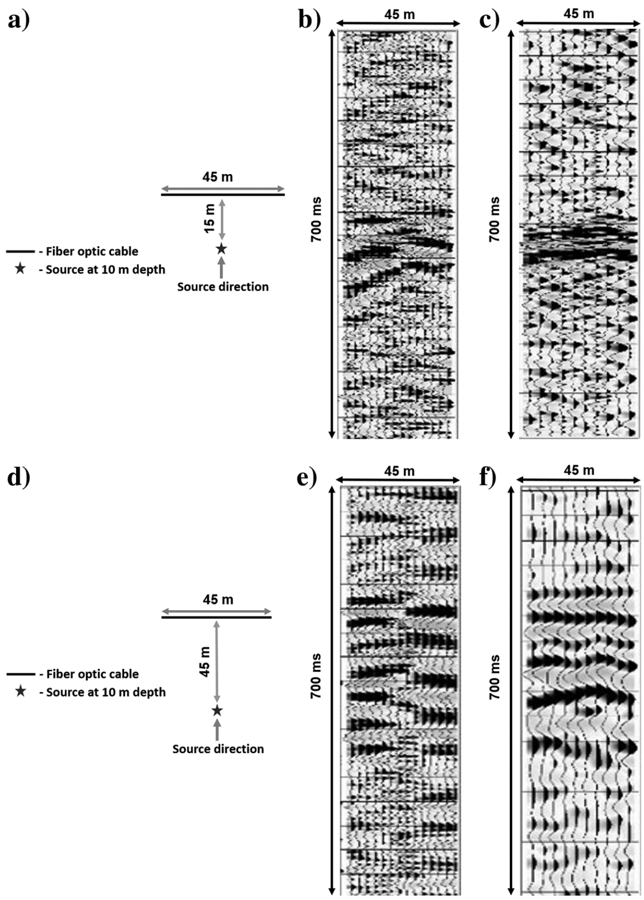

Figure 4. A comparison of DAS and geophone data. (a) A map view of the acquisition setup. The shot records correspond to the setup in (a) acquired with (b) DAS and (c) 5 Hz geophones. (d) A map view of the acquisition setup. The shot records correspond to the setup in (d) acquired with (e) DAS and (f) 5 Hz geophones.

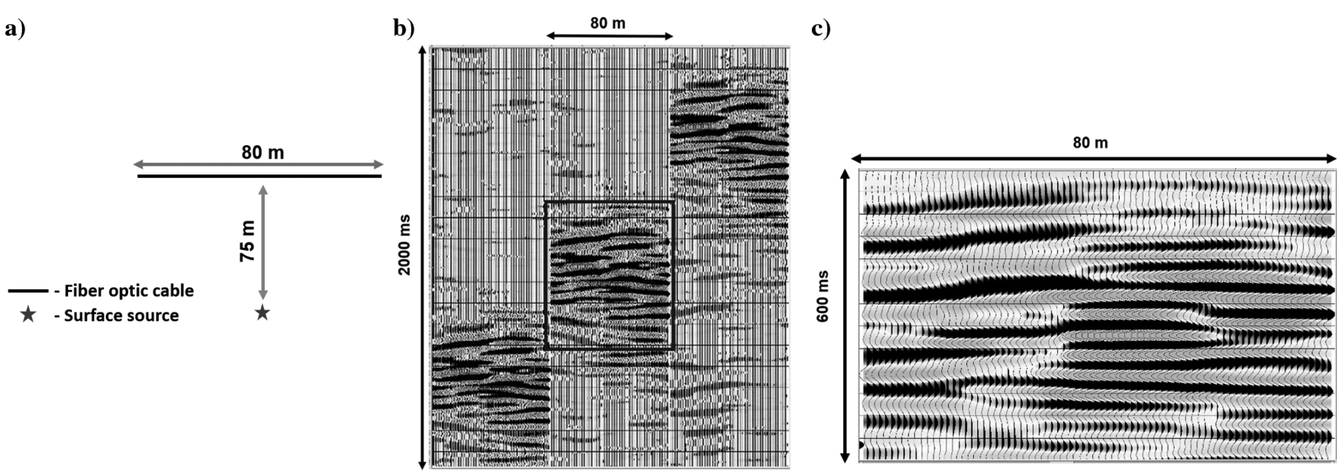

Figure 3. (a) A map view of the acquisition setup. (b) Three shot records acquired with a DAS array. (c) A magnification of one of the records indicated by the box in (b).

DOI:10.1190/geo2020-0400.1

DOI:10.1190/geo2020-0400.1

which are on the surface (see Figure 6a). The boreholes have a diameter of 10 cm and a depth of 45 m. They are located 15 m apart and filled with sand to ensure coupling. A 5 kg sledgehammer source was applied on the surface between points b and c. Figure 6b presents the nontriggered seismogram recorded along the a-d fiber. The low-frequency content of the data is similar to what we observed in the horizontal DAS experiments. A more detailed examination of only the left (a-b) borehole data is shown in Figure 6c. In spite of its low-frequency content, the signal can be traced over the entire length of the vertical fiber. One of the advantages of collecting data in boreholes is the ability to extract velocity information from checkshots. This velocity information is essential for accurately locating the voids. To verify the usability of the vertical DAS for this purpose, a checkshot calculation was tested. Figure 7a presents the picks on the seismogram acquired by the vertical DAS array, where the up or down part of the DAS array may be used. The calculated velocity function is plotted in Figure 7b. The values obtained from the checkshot are in agreement with the known velocity values in that area.

VOID IMAGING — FIELD DATA EXAMPLE

To check whether DAS is feasible for the application of imaging shallow subsurface voids, we conducted a 2D surface survey at area A, in the vicinity of a manmade elongated void. The 15 m deep void's long axis is perpendicular to the survey line and has a cross section of approximately 2 m tall × 1 m wide.

DAS data were acquired using a 5 kg sledgehammer as the source and a DAS array of 153 receiver stations with horizontal spacing of 1 m. The DAS array was deployed horizontally in a 0.5 m deep trench. In total, 120 shot locations were placed every 1 m along the receiver line. The first shot was applied at the first receiver location, and the last shot was applied at the location of receiver number 120 (see Figure 8a). Three shots were recorded at each shot location, and these were stacked to enhance the signal-to-noise ratio. A typical shot gather from the middle of the source line is displayed in Figure 8b. Although the void is right under the survey line, there is no way to observe the backscattered diffraction from the void.

We started our search for the void by applying the multichannel analysis of surface waves (MASW) method to the DAS data. MASW is a common method that uses the frequency-dependent properties of Rayleigh-type surface waves to estimate the shallow S-wave velocity (Park et al., 1999). Multichannel acquisition can assist in the task of void detection in two ways. First, for a given P-wave velocity, an S-wave velocity model can be estimated under the acquired seismic line. A subsurface void might manifest as an anomaly in the estimated S-wave velocity model. Second, when surface waves hit a subsurface void, their backscattered energy can be used by the backscattered analysis of surface waves method to determine the horizontal location of the void (Sloan et al., 2010, 2015). In this study, however, we only applied MASW to the DAS data.

During MASW processing, shot gathers were transformed into overtone images plotting the frequency versus the phase velocity. Then, dispersion curves were extracted for each shot location by picking the overtone images along their maximum amplitude (see Figure 9). Using a 2D P-wave velocity model, interpolated from two checkshots (see Figure 10), each dispersion curve was then inverted into a 1D S-wave velocity profile in 1 m intervals

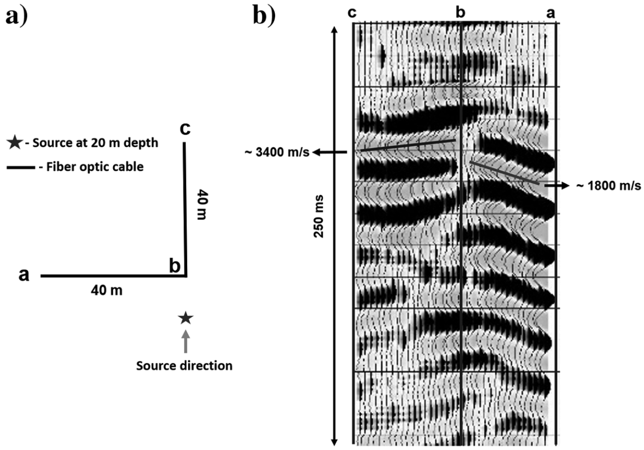

Figure 5. (a) A map view of the acquisition setup. (b) A recorded seismogram acquired by the DAS array.

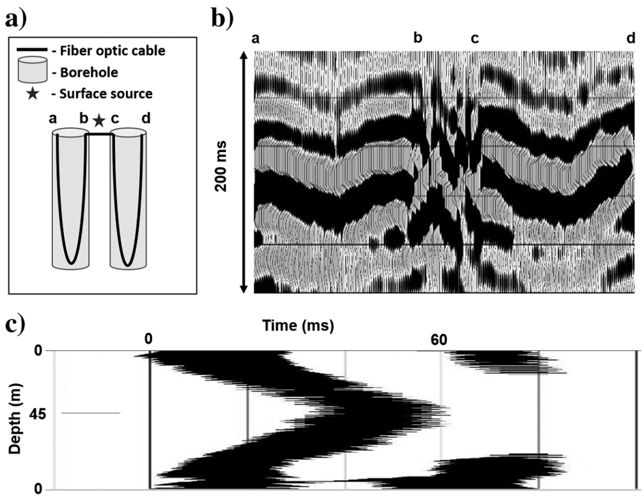

Figure 6. Data from a surface shot acquired with a DAS array in a borehole configuration. (a) Acquisition setup. (b) Surface shot recorded in two boreholes by the DAS borehole array. (c) Seismogram recorded by a single borehole (down and up) segment of the DAS array.

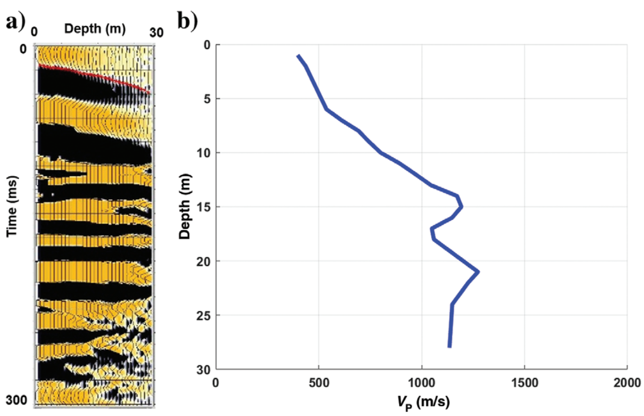

Figure 7. (a) A checkshot acquired by a vertical DAS array. First-break picking is denoted by the red line. (b) P-wave velocity model calculated from the checkshots.

(Xia et al., 1999). Finally, these 1D profiles were interpolated to obtain a 2D S-wave velocity model of the subsurface down to a depth of 22 m, which is the average penetration depth of all of the 1D profiles.

Figure 11 shows the interpolated 2D S-wave velocity model obtained from the MASW method. Ideally, the S-wave velocity should approach zero at the void location (see the red arrow in Figure 11 for the horizontal location of the void). Although the quality of the dispersion curves is good (see Figure 9), it is impossible to detect the void by the standard DAS-based MASW technique.

Diffraction imaging is a widely recognized tool for detecting subsurface heterogeneities and discontinuities that are smaller than the seismic wavelength (Khaidukov et al., 2004). Seismic diffractions may occur in the presence of faults, fractures, pinch-outs, dikes, and small scattering objects, such as boulders, cavities, karsts, and voids.

The diffraction imaging algorithm used here is based on the path-integral concept (Landa, 2004). Taking into account the fact that the estimated velocity is not accurate enough for applying a depth migration, we perform a kinematic path summation over a large range of constant-velocity ray trajectories. This velocity range is determined according to the velocities shown in Figures 10 and 11. The workflow that we used here is identical to the one suggested by Wechsler et al. (2020), in which the imaging procedure is carried out in the depth domain aiming to maximize energy along backscattered diffraction paths (Keydar and Landa, 2019). We used the entire set of 120 shot records recorded by the DAS system to construct

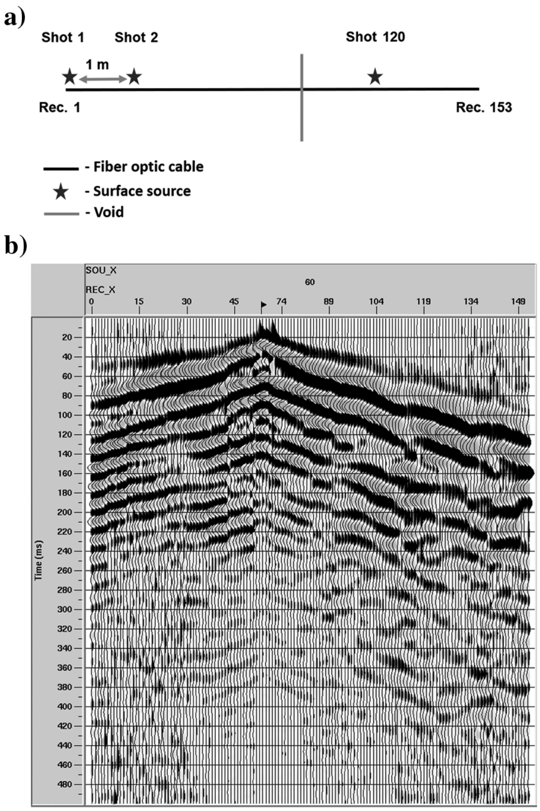

Figure 8. (a) A map view of the acquisition setup. (b) One of the 120 shot records, acquired with the DAS array, used as data for the MASW and shallow diffraction imaging.

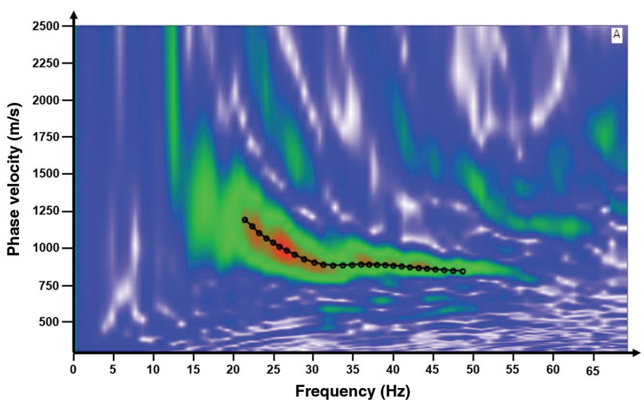

Figure 9. Example of an overtone image. The black circles denote a picked dispersion curve. Higher amplitudes are represented by warmer colors.

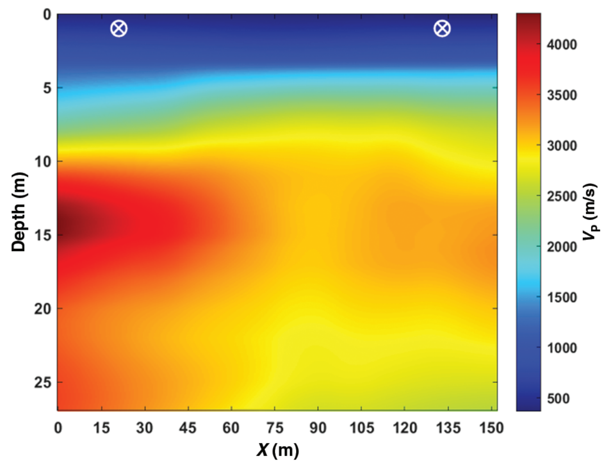

Figure 10. A 2D P-wave velocity model obtained from checkshots and used for the MASW inversion scheme. The borehole locations are denoted by the white circled crosses.

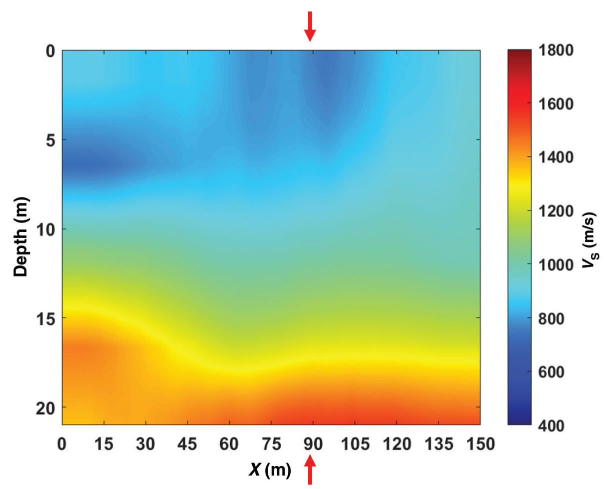

Figure 11. A 2D S-wave velocity model obtained by the MASW. The horizontal location of the void is denoted by the red arrows.

DOI:10.1190/geo2020-0400.1

DOI:10.1190/geo2020-0400.1

the diffraction summation image over the entire length of the fiber spread, down to a depth of 30 m. The size of each pixel in the calculated image was 0.5 × 0.5 m.

Figure 12 displays the resulting 2D diffraction image. The colors of the image represent a coherence measure (semblance in the applied algorithm) along a backscattered diffraction path from the image point. A very clear anomaly having the maximal semblance value can be seen at $x = 90$ m, with a depth of 16 m. The true location of the void is in the center of the anomaly. Hence, we can conclude that the diffraction imaging algorithm provided an accurate result.

DISCUSSION

Recent comparisons between geophone and DAS data are often considered to be successful if the DAS quality matches that of the geophones (e.g., Bakulin et al., 2019). For shallow seismic operations used for optimal void detection, such a comparison is essential because most commercially available DAS equipment has been traditionally optimized for the oil and gas industry or for earthquake seismology. In this study, we examined the possibility of using existing DAS technology for void detection in the shallow subsurface. The processing and analysis methods presented here have all been successfully tested before using geophones. Therefore, our main conclusion is that qualitatively similar results can be obtained with DAS.

The fundamental difference between these two types of sensors was expected to affect the analysis results. As a result, we conducted the field experiments in two very distinct test sites. Due to the known geologic complexity of the shallow subsurface, our initial tests will definitely need to be expanded upon, yet several conclusions can be drawn from our results. Although we focused our study on operations directly related to void detection, these conclusions are valid for many shallow-seismic investigations.

The first topic that we addressed was the frequency content. We demonstrated that the DAS data exhibit significantly lower frequencies compared with standard geophones. This observation depends on many parameters, such as fiber deployment, coupling, the natural frequency of geophones, and more. However, we do not see this limitation as a problem for the large variety of tested applications — from surface-waves analysis to a detailed checkshot study along a very shallow borehole.

Then, we considered the potential of wavefield separation. Earlier studies, all conducted with geophones, demonstrated the advantage of using S-waves for improved void detection and imaging. Unlike a geophone that can record data in all directions (e.g., a 3C geophone), the DAS system, using a standard fiber, provides a single-direction sensitivity. We showed that for specific subsurface source excitations, or in a similar way — backscattering from subsurface secondary sources, the distinct phase change along the sensing fiber could provide an initial estimate of the direction from the fiber to the source. A more challenging goal would be to kinematically separate the P- and S-wavefields, which would benefit the process of void detection. We managed to successfully obtain good separation by deploying an L-shaped FO cable. There is, of course, the big question about the practicality and cost of such a deployment. It is possible that a more advanced DAS system, for example, one that uses a helical fiber, will overcome this sensing limitation without the extra effort required for the deployment. Moreover, although the cost issue is outside the scope of this study, if we take into account the cost of the IU, the trenching, and the deployment of the fiber, it will obviously be more expensive than placing an array of geophones (surface or downhole) with a standard recording system. However, if an area has to be monitored for an extended period of time to detect voids (sinkholes, environmental changes, clandestine tunnels, etc.), mainly in urban places, a permanent fiber deployment may be more economical than a set of permanent geophones. A more plausible deployment is by setting the perpendicular fiber in the vertical direction into a borehole. Such a layout has already been presented on a larger scale (Bakulin et al., 2017). An encouraging conclusion comes from the fact that our usage of a standard DAS system, operated with a 10 m gauge length, did not affect our ability to analyze data along relatively short (40–50 m) and perpendicular (horizontal and vertical configurations) fiber segments.

The third subject that we focused on was velocity estimation. The accuracy of the velocity function in the vicinity of the void is essential for its imaging and localization. Standard procedures, such as a checkshot survey and MASW, were performed successfully using horizontal and vertical DAS data. Detecting the void by means of its strong effect on the S-wave velocity was not possible using the simple methods presented in this study. The size of the void, its depth of 15 m below the surface, and the low-frequency content of the DAS data are the main factors that prevented us from detecting the anomalous velocity near the void as suggested in other studies (Nolan et al., 2011, 2013; Sloan et al., 2013).

Finally, we performed shallow diffraction imaging to detect the void because a small void in the subsurface can be considered as a diffractor. When it is a straight tunnel, the void can be represented by a linear diffractor (Keydar and Landa, 2019). If only 2D data are available and the acquisition line crosses the void or its trajectory, the imaging task is to collapse the recorded diffracted energy into a point. When an accurate subsurface velocity is available, a standard prestack migration is recommended as the imaging procedure. Nonetheless, obtaining an accurate velocity model is often impossible for shallow seismic data. In addition, the diffracted energy may represent a mode-converted wave that combines P- and S-wave paths. Using a robust velocity analysis procedure, we were able to define a range of velocities for the path-summation method of diffraction imaging (Landa, 2004). We applied this summation over the entire range of the P- and S-wave velocities defined in the area. Although the diffracted signal from the void cannot be observed on the seismograms, the imaging result is very accurate. For better imaging of more complex voids or tunnels, multi-2D or even 3D data will be required. To simplify this imaging procedure, wavefield separation should be successfully applied. In this case, we should be able to calculate a few different images, based on the diffracted wavepaths (P-P, P-S, etc.). Subsequently, the correct position of the void can be confirmed by requiring all images to be focused

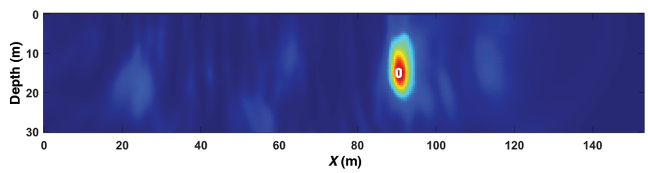

Figure 12. A 2D enhanced diffraction section. The true location of the void is indicated by the white rectangle. Higher semblance values are represented by warmer colors.

on the same subsurface location. At this point, such a separation is easy to perform with 3C geophones, whereas the simple fiber DAS will require complicated deployment to achieve this goal.

CONCLUSION

We successfully demonstrate the usage of standard DAS FO cables to acquire seismic data in the shallow subsurface. Most of the procedures presented here can be implemented for a wide range of shallow seismic investigations. We have shown that, even with conventional DAS equipment, a dense seismic survey can be successfully conducted, mainly for the purpose of void detection. Our observations suggest that separation of P- and S-waves appears to be possible using an appropriate deployment of perpendicular DAS arrays. Results establish that seismic data acquired by DAS can be effectively used to detect a subsurface void using shallow diffraction imaging. These data demonstrate that velocity analysis can be accomplished using conventional checkshot surveys and surface-wave inversion. Our findings indicate that a grid of perpendicular DAS arrays, including fibers in vertical boreholes, should provide high-quality DAS data that would be ideal for void detection and localization.

ACKNOWLEDGMENTS

We would like to thank P. Sinitsyn, O. Shamir, and G. Tzarfati for their hard work in the field. In addition, we wish to thank A. Lellouch, H. Marcus, and L. Abukrat for their helpful comments and fruitful discussions. The authors wish to thank the editors and the anonymous reviewers for their excellent critiques and suggestions that greatly improved the paper.

DATA AND MATERIALS AVAILABILITY

Data associated with this research are confidential and cannot be released.

DOI:10.1190/geo2020-0400.1

REFERENCES

Auken, E., L. Pellerin, N. B. Christensen, and K. Sørensen, 2006, A survey of current trends in near-surface electrical and electromagnetic methods: Geophysics, **71**, no. 5, G249–G260, doi: 10.1190/1.2335575.

Bakulin, A., P. Golikov, R. Smith, K. Erickson, I. Silvestrov, and M. Al-Ali, 2017, Smart DAS upholes for simultaneous land near-surface characterization and subsurface imaging: The Leading Edge, **36**, 1001–1008, doi: 10.1190/tle36121001.1.

Bakulin, A., P. Golikov, R. Smith, K. Erickson, I. Silvestrov, and M. Al-Ali, 2019, Smart DAS uphole acquisition system for near surface characterization and imaging: 88th Annual International Meeting, SEG, Expanded Abstracts, 201–205, doi: 10.1190/segam2018-2995883.1.

Barkved, O., B. Bartman, B. Compani, J. Gaiser, R. Van Dok, T. Johns, P. Kristiansen, T. Probert, and M. Thompson, 2004, The many facets of multicomponent seismic data: Oilfield Review, **16**, 42–56.

Belfer, I., I. Bruner, S. Keydar, A. Kravtsov, and E. Landa, 1998, Detection of shallow objects using refracted and diffracted seismic waves: Journal of Applied Geophysics, **38**, 155–168, doi: 10.1016/S0926-9851(97)00025-6.

Butler, D. K., 1984, Microgravimetric and gravity gradient techniques for detection of subsurface cavities: Geophysics, **49**, 1084–1096, doi: 10.1190/1.1441723.

Cassidy, N. J., R. Eddies, and S. Dods, 2011, Void detection beneath reinforced concrete sections: The practical application of ground-penetrating radar and ultrasonic techniques: Journal of Applied Geophysics, **74**, 263–276, doi: 10.1016/j.jappgeo.2011.06.003.

Daley, T. M., B. M. Freifeld, J. Ajo-Franklin, S. Dou, R. Pevzner, V. Shulakova, S. Kashikar, D. E. Miller, J. Goetz, J. Henninges, and S. Lueth, 2013, Field testing of fiber-optic distributed acoustic sensing (DAS) for subsurface seismic monitoring: The Leading Edge, **32**, 699–706, doi: 10.1190/tle32060699.1.

Dankbaar, J. W. M., 1987, Vertical seismic profiling — Separation of P- and S-waves: Geophysical Prospecting, **35**, 803–814, doi: 10.1111/j.1365-2478.1987.tb02259.x.

Dou, S., N. Lindsey, A. M. Wagner, T. M. Daley, B. Freifeld, M. Robertson, J. Peterson, C. Ulrich, E. R. Martin, and J. B. Ajo-Franklin, 2017, Distributed acoustic sensing for seismic monitoring of the near surface: A traffic-noise interferometry case study: Scientific Reports, **7**, 1–12, doi: 10.1038/s41598-017-11986-4.

Greenhalgh, S. A., I. M. Mason, E. Lucas, D. Pant, and R. T. Eames, 1990, Controlled direction reception filtering of P- and S-waves in τ-P space: Geophysical Journal International, **100**, 221–234, doi: 10.1111/j.1365-246X.1990.tb02482.x.

Karrenbach, M., D. Kahn, S. Cole, A. Ridge, K. Boone, J. Rich, K. Silver, and D. Langton, 2017, Hydraulic-fracturing-induced strain and microseismic using in situ distributed fiber-optic sensing: The Leading Edge, **36**, 837–844, doi: 10.1190/tle36100837.1.

Kendall, R., S. Jin, S. Ronen, and K. De Meersman, 2005, An SVD-polarization filter for ground roll attenuation on multicomponent data: 75th Annual International Meeting, SEG, Expanded Abstracts, 928–931, doi: 10.3997/2214-4609-pdb.17.A18.

Keydar, S., and E. Landa, 2019, Wave refocusing for linear diffractor using the time-reversal principle: Geophysical Prospecting, **67**, 1345–1353, doi: 10.1111/1365-2478.12784.

Khaidukov, V., E. Landa, and T. J. Moser, 2004, Diffraction imaging by focusing-defocusing: An outlook on seismic superresolution: Geophysics, **69**, 1478–1490, doi: 10.1190/1.1836821.

Lai, W. W. L., R. K. W. Chang, and J. F. C. Sham, 2018, A blind test of nondestructive underground void detection by ground penetrating radar (GPR): Journal of Applied Geophysics, **149**, 10–17, doi: 10.1016/j.jappgeo.2017.12.010.

Landa, E., 2004, Imaging without a velocity model using path-summation approach: 74th Annual International Meeting, SEG, Expanded Abstracts, 1818–1821, doi: 10.1190/1.1845174.

Lellouch, A., and M. Reshef, 2017, Shallow diffraction imaging in an SH-wave crosshole configuration: Geophysics, **82**, no. 1, S9–S18, doi: 10.1190/geo2016-0154.1.

Lellouch, A., S. Yuan, Z. Spica, B. Biondi, and W. L. Ellsworth, 2019, Seismic velocity estimation using passive downhole distributed acoustic sensing records: Examples from the San Andreas fault observatory at depth: Journal of Geophysical Research, Solid Earth, **124**, 6931–6948, doi: 10.1029/2019JB017533.

Lindsey, N. J., E. R. Martin, D. S. Dreger, B. Freifeld, S. Cole, S. R. James, B. L. Biondi, and J. B. Ajo-Franklin, 2017, Fiber-optic network observations of earthquake wavefields: Geophysical Research Letters, **44**, 11,792–11,799, doi: 10.1002/2017GL075722.

Martin, E. R., C. M. Castillo, S. Cole, P. S. Sawasdee, S. Yuan, R. Clapp, M. Karrenbach, and B. L. Biondi, 2017, Seismic monitoring leveraging existing telecom infrastructure at the SDASA: Active, passive, and ambient-noise analysis: The Leading Edge, **36**, 1025–1031, doi: 10.1190/tle36121025.1.

Mateeva, A., J. Lopez, J. Mestayer, P. Wills, B. Cox, D. Kiyashchenko, Z. Yang, W. Berlang, R. Detomo, and S. Grandi, 2013, Distributed acoustic sensing for reservoir monitoring with VSP: The Leading Edge, **32**, 1278–1283, doi: 10.1190/tle32101278.1.

Mateeva, A., J. Lopez, H. Potters, J. Mestayer, B. Cox, D. Kiyashchenko, P. Wills, S. Grandi, K. Hornman, B. Kuvshinov, W. Berlang, Z. Yang, and R. Detomo, 2014, Distributed acoustic sensing for reservoir monitoring with vertical seismic profiling: Geophysical Prospecting, **62**, 679–692, doi: 10.1111/1365-2478.12116.

Mestayer, J., B. Cox, P. Wills, D. Kiyashchenko, J. Lopez, M. Costello, S. Bourne, G. Ugueto, R. Lupton, G. Solano, D. Hill, and A. Lewis, 2011, Field trials of distributed acoustic sensing for geophysical monitoring: 81st Annual International Meeting, SEG, Expanded Abstracts, 4253–4257, doi: 10.1190/1.3628095.

Nolan, J. J., R. Miller, J. Ivanov, S. Peterie, and E. Lindgren, 2013, Near-surface salt dissolution void identification using passive MASW: 83rd Annual International Meeting, SEG, Expanded Abstracts, 2212–2217, doi: 10.1190/segam2013-1146.1.

Nolan, J. J., S. D. Sloan, S. W. Broadfoot, J. R. McKenna, and O. M. Metheny, 2011, Near-surface void identification using MASW and refraction tomography techniques: 81st Annual International Meeting, SEG, Expanded Abstracts, 1401–1405, doi: 10.1190/1.3627464.

Park, C. B., R. D. Miller, and J. Xia, 1999, Multichannel analysis of surface waves: Geophysics, **64**, 800–808, doi: 10.1190/1.1444590.

Parker, T., S. Shatalin, and M. Farhadiroushan, 2014, Distributed acoustic sensing — A new tool for seismic applications: First Break, **32**, 61–69, doi: 10.3997/1365-2397.2013034.

Peterie, S. L., R. D. Miller, J. Ivanov, and S. D. Sloan, 2020, Shallow tunnel detection using SH-wave diffraction imaging: Geophysics, **85**, no. 2, EN29–EN37, doi: 10.1190/geo2018-0731.1.

Rybakov, M., V. Goldshmidt, L. Fleischer, and Y. Rotstein, 2001, Cave detection and 4-D monitoring: A microgravity case history near the Dead Sea: The Leading Edge, **20**, 896–900, doi: 10.1190/1.1487303.
Shustak, M., N. Wechsler, A. Yurman, and M. Reshef, 2015, Comparison of surface vs. cross-hole seismic methods for void detection in the shallow sub-surface: 85th Annual International Meeting, SEG, Expanded Abstracts, 2286–2291, doi: 10.1190/segam2015-5900317.1.
Sloan, S. D., J. J. Nolan, S. W. Broadfoot, J. R. McKenna, and O. M. Metheny, 2013, Using near-surface seismic refraction tomography and multichannel analysis of surface waves to detect shallow tunnels: A feasibility study: Journal of Applied Geophysics, **99**, 60–65, doi: 10.1016/j.jappgeo.2013.10.004.
Sloan, S. D., S. L. Peterie, J. Ivanov, R. D. Miller, and J. R. McKenna, 2010, 12. Void detection using near-surface seismic methods, *in* R. D. Miller, J. D. Bradford, and K. Holliger, eds., Advances in near-surface seismology and ground-penetrating radar: SEG, SEG Geophysical Developments Series 15, 201–218.
Sloan, S. D., S. L. Peterie, R. D. Miller, J. Ivanov, J. T. Schwenk, and J. R. McKenna, 2015, Detecting clandestine tunnels using near-surface seismic techniques: Geophysics, **80**, no. 5, EN127–EN135, doi: 10.1190/geo2014-0529.1.
Wang, Y., S. C. Singh, and P. J. Barton, 2002, Separation of P- and SV-wavefields from multi-component seismic data in the τ-p domain: Geophysical Journal International, **151**, 663–672, doi: 10.1046/j.1365-246X.2002.01797.x.
Wechsler, N., M. Shustak, and E. Ben-Yosef, 2020, Diffraction stack imaging as a potential tool for detecting underground voids — The case of the ancient copper mines of Timna Valley (Israel): Archaeological Prospection, **27**, 27–37, doi: 10.1002/arp.1754.
Xia, J., R. D. Miller, and C. B. Park, 1999, Estimation of near-surface shear-wave velocity by inversion of Rayleigh waves: Geophysics, **64**, 691–700, doi: 10.1190/1.1444578.

Biographies and photographs of the authors are not available.

DOI:10.1190/geo2020-0400.1